

The Oxidation of Hydrazobenzene Catalyzed by Cobalt Complexes in Nonaqueous Solvents

Stephen S. B. Kim,* Roger B. Hommer, and Roderick D. Cannon†

Department of Chemistry, University of Ulsan, Ulsan 690, P.O. Box 18, Korea. *E-mail: sbkim41@hotmail.com

†School of Chemical Sciences, University of East Anglia, Norwich, NR4 7TJ, England, U.K.

Received August 15, 2005

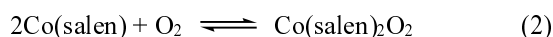
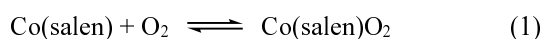
The oxidation of hydrazobenzene by molecular oxygen in the polar solvent methanol is catalysed by a Schiff's base complex Co(3MeOsalen) which is a synthetic oxygen carrier. The products are *trans*-azobenzene and water. The rate of the reaction has been studied spectrophotometrically and the rate law established. A mechanism involving a ternary complex of catalyst, hydrazobenzene and molecular oxygen has been proposed. The kinetic studies show that a ternary complex CoL·H₂AB·O₂ is involved in the rate determining step. The reactions are summarised in a catalytic cycle. The kinetic data suggest that a ternary complex involving Co(3MeOsalen), triphenyl-phosphine and molecular oxygen is catalytically active species but at higher triphenyl-phosphine concentrations the catalyst becomes inactive. The destruction of the catalytic activity could be due to the catalyst becoming coordinated with triphenyl phosphine at both z axis sites of the complex *e.g.* Co(3MeOsalen)(PPh₃)₂.

Key Words : Catalytic cycle, Cobalt complexes, Hydrazobenzene, Axial ligands, Reaction mechanisms

Introduction

It has been known since the observation of Pfeiffer and his co-workers¹ in 1933 that Cobalt(II) Schiff's base complexes *e.g.* *N,N'*-ethylenebis(salicylideneiminato)-cobalt(II), Co(salen), Figure 1, form reversible complexes with oxygen. Tsumaki² in 1938 demonstrated that the colour change observed upon exposing Co(salen) to air as due to the reversible oxygenation of complexes, as shown in equations (1) and (2).

Although molecular oxygen reacts reversibly with some metal complexes, there are certain complexes formed



irreversibly such as [(Co(NH₃)₅)₂O₂](SCN)₄.³

A study of synthetic dioxygen complexes is important for understanding the bonding of dioxygen to transition metal complexes and the effect of this bonding upon the reactivity of dioxygen toward other substrates.

There has been considerable recent interest in these compounds because of their relationship to the natural iron-containing oxygen carriers hemoglobin and myoglobin.³ Hemoglobin and myoglobin consist of an iron-porphyrin complex, the haem group, embedded in the protein which provides one axial ligand, an imidazole group, to the iron. On oxygenation the sixth coordination site of the iron accepts the dioxygen ligand.

Thus the ligand field about the iron in oxyhemoglobin is approximately octahedral.⁴ Reversible dioxygen complexes are utilised in living organism for the transport and storage⁵ of molecular oxygen. Dioxygen binding also occurs in enzymes which catalyse oxidation processes.⁶

Cobalt(II) Schiff's base complexes are square planar with

a low spin d⁷ electron configuration. The binding of an axial, fifth ligand leads to a ground state with the unpaired electron in the d_{z²} orbital. This electron configuration is a necessary prerequisite for the binding of dioxygen.⁷ Drago and Corden,⁸ in their spin-pairing model for the binding of dioxygen, presented evidence that the odd electron in the oxygenated complex is in the dioxygen π* orbital, but that the extent of electron transfer from cobalt to oxygen is dependent on the nature of the equatorial and axial ligands. In the extreme case of complete electron transfer the complex could be formulated as cobalt(III)-superoxide.

The change in the electronic structure of oxygen from the relatively unreactive triplet ground state to a doublet coordinated species, with a weakened O-O bond bearing fractional negative charge, could be expected to enhance the reactivity of oxygen in radical or nucleophilic reactions.

In recent years the catalytic behavior of dioxygen complexes, Cobalt(II) Schiff base oxygen carrier complexes have been studied by both academics and industrialist.⁶ Cobalt(II) Schiff's base complexes with added axial ligands have been shown to catalyse the oxidation by oxygen of secondary alcohols⁹ to ketones, and of phenols¹⁰ to quinones.

Cobalt complexes with salen or polyamines and related ligands have been employed as catalysts.^{11,12} Savitskii⁹ has made a kinetic study of the catalytic oxidation of isopropanol to acetone using initial reaction rates from oxygen consumption, and they have derived the rate law. They have also published a kinetic study of the catalytic oxidation of hydroquinone¹³ in presence of Co(salen) in dimethylacetamide (DMA). They identified the main product of the oxidation of hydroquinone as *p*-benzoquinone. Nishinaga¹¹ indicated that a better model for natural systems is the catalytic double bond oxidation.^{3,11} Nishinaga *et al.*¹⁴ have

reported that the oxidation of 2,6-di-*t*-butylphenols by five-coordinate Co(II)Schiff-base complexes, for example cobalt(II)bis(salicylideneamino)propylamine, has been found to result in the formation of peroxyquinolatocobalt(III) complexes. Drago *et al.*^{10,15} began a kinetic investigation to provide insight into both the oxidation of 2,6-dimethylphenol and the deactivation of the catalyst CoSMDPT, cobalt(II)(3-salicylideneaminopropyl)methylamine. They also reported the catalytic oxidation¹⁶ of olefins by molecular oxygen and by using CoSalMDPT, cobalt(II)-bis(salicylidene-iminopropyl)methylamine. It is interesting to note that the catalyst CoSalMDPT demonstrates some substrate selectivity, oxidising linear olefins but not cyclohexane, and the reaction rate is independent of O₂ pressure.

The structurally related bis(dimethylglyoximato)cobalt(II) has been reported to catalyse the oxidation of hydrazobenzene to azobenzene in the presence of triphenylphosphine.¹⁷ Kinetic studies^{9,10} have shown that in the oxidation of alcohols and phenols the transition state is a ternary complex of dioxygen, cobalt catalyst (including axial base) and substrate. Thus the reactions resemble an enzyme-catalysed process in which the two substrates, dioxygen and the organic molecule, are brought together by the catalyst.

In this paper we show that the oxidation of hydrazobenzene catalysed by Co(3MeOsalen), Figure 1, follows a similar kinetic scheme, providing evidence of saturation of the catalyst by the substrate as an enzyme catalysed reaction. Autoxidation of hydrazobenzene was first described in 1901 by Manchot and Herzog.¹⁸ This, and later work^{19,20} has shown that the products are *trans*-azobenzene and hydrogen peroxide with the reaction first order in hydrazobenzene and oxygen.

Results and Discussion

Studies of the oxidation of organic substrates catalysed by transition metal complexes have been focussed on three main themes: (1) the discovery of new oxidation catalysts and new catalytic oxidation reactions, (2) the elucidation of mechanisms through kinetic studies, and (3) the tailoring of the catalyst and reaction conditions for maximum catalytic activity.²¹ Our work concentrates on the second of these.

Co(II)(3MeOsalen) has been used as a catalyst in the oxidation of hydrazobenzene (H₂AB). Hydrazobenzene is

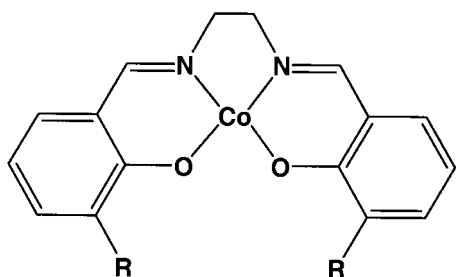


Figure 1. Cobalt(II)-Schiff base complexes, *e.g.* *N,N'*-ethylenebis(salicylideneiminato)-cobalt(II), Co^{II}(salen), R = H, Co(salen); R = CH₃O, Co(3MeOsalen).

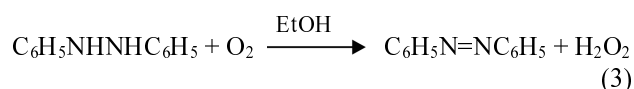
catalytically oxidised to azobenzene (AB) by L·Co(3MeOsalen)·O₂ (L = Ligand) in the polar solvent, methanol. Azobenzene has two isomers (*cis* and *trans*), thus the product of oxidation may provide stereochemical information about the reaction pathway. Hydrazobenzene is readily autoxidised to azobenzene and hydrogen peroxide,¹⁸ and there is a possibility that the hydrogen peroxide produced may also oxidise hydrazobenzene. The rates of the oxidation of hydrazobenzene are measured under O₂ and air saturation at the 315 nm or 437 nm absorption bands of azobenzene.

The solvent methanol has a high polarity and the oxidation reaction may be carried out with or without an axial ligand. However, ligands were employed to observe their effect on the catalytic activity.

The results and discussion have been split into two parts: the kinetics of the Co(II)(3MeOsalen) catalysed oxidation of hydrazobenzene, and the reaction mechanism of hydrazobenzene oxidation.

The term autoxidation²² is applied generally to oxidations which can be effected by free oxygen (*e.g.* by air) at moderate temperatures and may be contrasted with the rapid processes of combustion which require high temperatures. It has long been known that autoxidations are promoted by light²³ and by small quantities of many catalysts.

The autoxidation of hydrazobenzene has already been well studied.¹⁸ Hydrazobenzene is readily autoxidised in ethanol with the formation of azobenzene and hydrogen peroxide.¹⁹ They found that in an alcoholic solution the reaction is practically quantitative, equation (3).



The rate of the autoxidation of hydrazobenzene in methanol was found to be first order in substrate at room temperature.²¹ Hinshelwood and Blackadder²⁴ reported that autoxidation of hydrazobenzene in alkaline solution (44% ethanol) containing oxygen was “a spontaneous reaction of first order with respect to hydrazobenzene”. The rate of reaction became independent of oxygen once a concentration about 5% oxygen had been exceeded in the atmosphere to which the solution had been exposed. Savitskii and Nelyubin¹³ demonstrated that the rate of O₂ consumption in the oxidation of hydroquinone is independent of oxygen pressure at 1 atmosphere.

When the initial rate *R*₀ is plotted against the hydrazobenzene concentration, the plots are linear, Figure 2. We have demonstrated that autoxidation of hydrazobenzene in anhydrous methanol was found to be first order in O₂ or air, Table 1. The rate constants of the reaction mixture were calculated to be 3.85 × 10⁻⁶ sec⁻¹ in the O₂ saturated methanol and 1.98 × 10⁻⁶ sec⁻¹ in the air saturated methanol. The rates of the autoxidation are used to find the initial rates in the catalysed reaction in Table 2 and 3.

The product azobenzene has two isomers, *cis*- and *trans*-azobenzene.²⁵ *Trans*-azo-benzene is found to be planar, or at least peri-planar, while the phenyl rings of the *cis*-isomer are

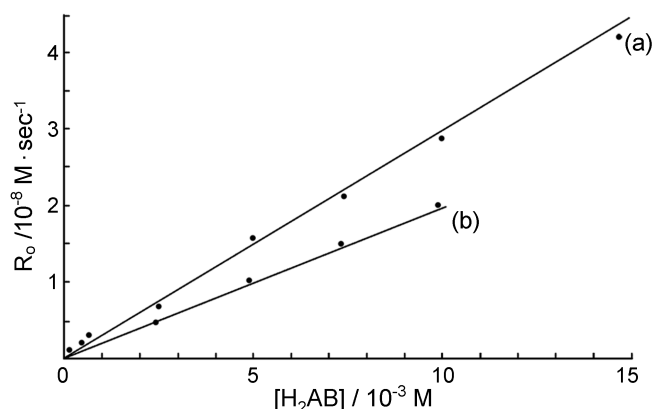


Figure 2. Plots of initial rates R_0 against $[H_2AB]$. O_2 (a) and air (b) saturated methanol at 25.0 °C, $\lambda = 315$ nm and 437 nm. The rate constants are $k(O_2) = 3.85 \times 10^{-6} \text{ sec}^{-1}$ and $k(\text{air}) = 1.98 \times 10^{-6} \text{ sec}^{-1}$.

Table 1. Effect of varying hydrazobenzene concentration, $[H_2AB]$ on the autoxidation of hydrazobenzene in O_2 and air saturated methanol at 25.0 °C

NO.	$[H_2AB] / 10^{-3} \text{ M}$	O_2 saturated methanol		air saturated methanol	
		$(dA/dt)_0 / 10^{-5} \text{ sec}^{-1}$	$R_0 / 10^{-8} \text{ sec}^{-1}$	$(dA/dt)_0 / 10^{-5} \text{ sec}^{-1}$	$R_0 / 10^{-8} \text{ sec}^{-1}$
1	0.102	0.667	0.0469		
2	0.388	2.29	0.161 ^a		
3	0.411	3.05	0.215 ^b		
4	2.45	10.0	0.704	7.02	0.494
5	4.90	22.6	1.59	14.0	0.986
6	7.35	30.1	2.12	21.1	1.49
7	9.80	41.4	2.91	28.1	1.98
8	14.7	60.0	4.22		

^aFrom Table 7. ^bFrom Table 8, $\lambda = 315$ nm ($\epsilon_{315} = 1.61 \times 10^4 \text{ M}^{-1} \cdot \text{cm}^{-1}$ (No. 1-3) and $\lambda = 437$ nm ($\epsilon_{437} = 5.09 \times 10^2 \text{ M}^{-1} \cdot \text{cm}^{-1}$ (No. 4-8). $\Delta\epsilon^{-1} = 7.04 \times 10^{-5} \text{ M} \cdot \text{cm}$. $R_0 = \Delta\epsilon_{315}^{-1} \cdot (dA/dt)_0$.

Table 2. Effect of varying hydrazobenzene concentration, $[H_2AB]$ on the oxidation of hydrazobenzene in O_2 saturated methanol at 25.0 °C

$[H_2AB] / 10^{-3} \text{ M}$	$(dA/dt)_0 / 10^{-3} \text{ sec}^{-1}$	$R_0^a / 10^{-7} \text{ M} \cdot \text{sec}^{-1}$	$R_0^b / 10^{-8} \text{ M} \cdot \text{sec}^{-1}$	$R_0 / 10^{-7} \text{ M} \cdot \text{sec}^{-1}$	$k_{0-1} / 10^1 \text{ sec}$	$[H_2AB]^{-1} / 10^2 \text{ M}^{-1}$
1.81	3.11	2.19	0.550	2.13	3.49	5.52
3.61	5.29	3.73	1.07	3.62	2.05	2.77
7.22	9.45	6.65	2.15	6.44	1.15	1.39
9.03	12.0	8.47	2.67	8.20	0.906	1.11
10.8	13.0	9.18	3.18	8.86	0.839	0.923
12.6	13.6	9.58	3.71	9.21	0.807	0.791
14.4	14.9	10.5	4.23	10.1	0.734	0.693

R_0^a : initial rate of the reaction mixture, R_0^b : initial rate on the autoxidation of H_2AB (from Figure 2), $R_0 = R_0^a - R_0^b$, $k_{0-1} = [Co(3MeOsalen)]/R_0$; $[Co(3MeOsalen)] = 7.43 \times 10^{-6} \text{ M}$, $\lambda = 315$ nm ($\epsilon(H_2AB) = 1.89 \times 10^3 \text{ M}^{-1} \cdot \text{cm}^{-1}$, $\epsilon(AB) = 1.61 \times 10^4 \text{ M}^{-1} \cdot \text{cm}^{-1}$), $R_0 = \Delta\epsilon^{-1} (dA/dt)_0$; $\Delta\epsilon^{-1} = 7.04 \times 10^{-5} \text{ M} \cdot \text{cm}$.

twisted (by 56°) out of the plane, Figure 3. *Trans*-azobenzene has been calculated (by the self-consistent field (SCF) method) to be more stable by 43.5 K·J·mol⁻¹ (10.4 Kcal·mol⁻¹) than the *cis*-isomer, which is in good agreement with the

Table 3. Effect of varying hydrazobenzene concentration, $[H_2AB]$ on the oxidation of hydrazobenzene in air saturated methanol at 25.0 °C

$[H_2AB] / 10^{-3} \text{ M}$	$(dA/dt)_0 / 10^{-3} \text{ sec}^{-1}$	$R_0^a / 10^{-7} \text{ M} \cdot \text{sec}^{-1}$	$R_0^b / 10^{-8} \text{ M} \cdot \text{sec}^{-1}$	$R_0 / 10^{-7} \text{ M} \cdot \text{sec}^{-1}$	$k_{0-1} / 10^1 \text{ sec}$	$[H_2AB]^{-1} / 10^2 \text{ M}^{-1}$
1.16	0.619	0.436	0.230	0.413	18.0	8.62
2.32	1.24	0.871	0.470	0.824	9.02	4.31
3.48	1.75	1.23	0.700	1.16	6.41	2.87
4.56	2.30	1.62	0.910	1.53	4.86	2.19
5.70	2.93	2.06	1.15	1.95	3.81	1.75
6.84	3.25	2.29	1.37	2.15	3.46	1.46
7.98	3.85	2.71	1.60	2.55	2.91	1.25
9.12	4.33	3.05	1.83	2.87	2.59	1.09
10.3	4.93	3.47	2.05	3.26	2.28	0.975

R_0^a : initial rate of the reaction mixture, R_0^b : initial rate on the autoxidation of H_2AB (from Figure 2), $R_0 = R_0^a - R_0^b$, $k_{0-1} = [Co(3MeOsalen)]/R_0$; $[Co(3MeOsalen)] = 7.43 \times 10^{-6} \text{ M}$, $\lambda = 315$ nm ($\epsilon(H_2AB) = 1.89 \times 10^3 \text{ M}^{-1} \cdot \text{cm}^{-1}$, $\epsilon(AB) = 1.61 \times 10^4 \text{ M}^{-1} \cdot \text{cm}^{-1}$), $R_0 = \Delta\epsilon^{-1} (dA/dt)_0$; $\Delta\epsilon^{-1} = 7.04 \times 10^{-5} \text{ M} \cdot \text{cm}$.

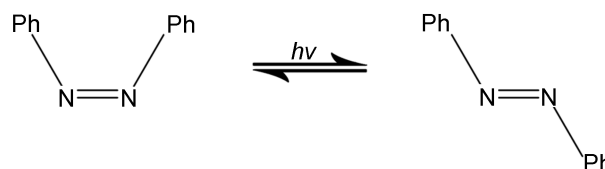


Figure 3. *Cis*- and *trans*-azobenzene (Ph : phenyl).

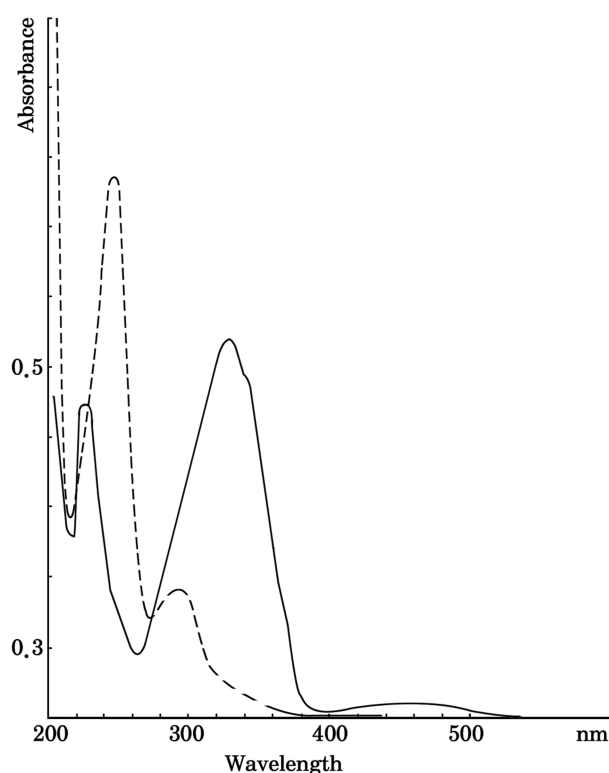


Figure 4. Absorption spectra of hydrazobenzene, broken curve, concentration $3.45 \times 10^{-2} \text{ M}$ and *trans*-azobenzene (solid curve, $2.75 \times 10^{-3} \text{ M}$). Methanol, 25 °C.

experimental value of 41.8 K·J·mol⁻¹ (10 Kcal·mol⁻¹).

Absorption spectra of hydrazobenzene (H_2AB) and *trans*-

Table 4. Absorption maxima of hydrazobenzene, *trans*-azobenzene, and *cis*-azobenzene. Methanol, 25.0 °C

Hydrazobenzene (H ₂ AB)		<i>Trans</i> -azobenzene (<i>trans</i> -AB)		<i>Cis</i> -azobenzene (<i>cis</i> -AB)	
λ_{\max} (nm)	ϵ (10 ³ M ⁻¹ ·cm ⁻¹)	λ_{\max} (nm)	ϵ (10 ³ M ⁻¹ ·cm ⁻¹)	λ_{\max} (nm)	ϵ (10 ³ M ⁻¹ ·cm ⁻¹)
245	21.8	227	13.1	240	> 8.61
289	5.23	315	16.1	298	> 6.42
(315)	(1.89)	(437)	(0.509)	425	> 1.36

Table 5. Further addition of hydrazobenzene to the reaction mixture

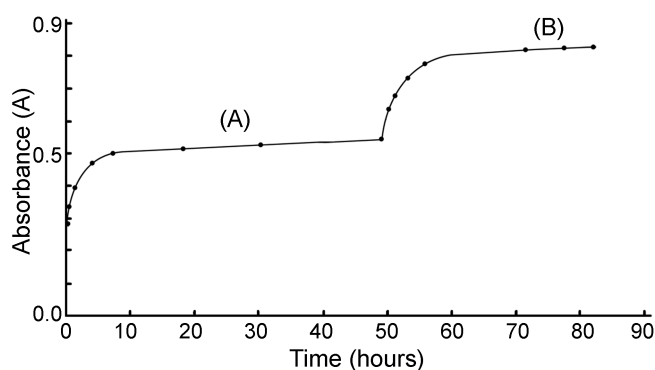
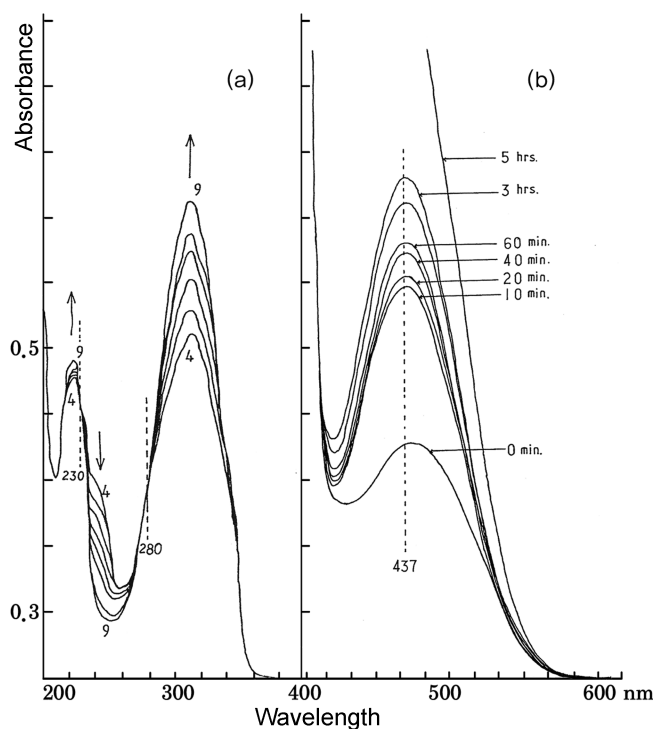
Time (hour)	Absorbance	Time (hour)	Absorbance
0	0.132	0 (49.8 hrs.)	0.620
0.183	0.223	0.117	0.625
0.417	0.290	0.217	0.626
0.767	0.337	0.517	0.636
1.58	0.339	1.48	0.670
2.67	0.445	2.48	0.696
4.17	0.478	3.57	0.719
6.67	0.496	6.15	0.772
18.5	0.509	22.4	0.809
21.7	0.524	28.2	0.822
24.2	0.523	35.1	0.825
30.5	0.536		
49.8	0.538		

At time = 49.8 hrs., a further addition of hydrazobenzene (0.4606 g to 50 mL solution) (5.00×10^{-2} M) to the reaction mixture. O₂ saturated methanol, 25.0 °C, $\lambda = 437$ nm, [Co(3MeOsalen)] = 5.24×10^{-4} M, [H₂AB] = 1.01×10^{-1} M.

azobenzene (AB) in methanol was recorded over the range of 600-200 nm, Figure 4. There are two bands observed at 245 nm and 289 nm. Extinction coefficients for these and of *cis*-azobenzene are given in Table 4.

Some *cis*-azobenzene was produced from *trans*-azobenzene (8.16×10^{-3} M) in methanol at 25.0 °C by irradiating it for about three hours at 315 nm in the cell compartment of a Farrand spectrofluorometer with 20 nm slits. Each isomer of azobenzene has three bands. Two of the bands in *trans*-azobenzene was shifted to shorter wavelengths in the *cis* isomer, Table 4. The absorption spectrum of the isomers in methanol is similar to that of *trans*-azobenzene in ethanol. The extinction coefficients in Table 4 are exact as conversion to the *cis* isomer has not reached 100%. During irradiation there was a large change in the absorbance of the bands at 315 nm and 437 nm in the first half hour, the rate of which decreased rapidly until after 21/2 hours, after which there was no further change in the absorbance. If during the course of the oxidation of hydrazobenzene in methanol, *cis*-azobenzene were formed as an intermediate, a band at 425 nm (literature 433 nm in ethanol)²⁶ should have been formed before the formation of the band at 437 nm due to *trans*-azobenzene.

The oxidation of hydrazobenzene (1.01×10^{-1} M) catalysed by Co(3MeOsalen) (5.24×10^{-4} M) produced *trans*-azobenzene as witnessed by a band at 437 nm in methanol at

**Figure 5.** Plot of absorbance, A, against time. O₂ saturated methanol, 25.0 °C, $\lambda = 437$ nm. [Co(3MeOsalen)] = 5.24×10^{-4} M. (A): [H₂AB] = 1.01×10^{-1} M (initially); (B): [H₂AB] = 0.500×10^{-1} M (0.4606 g to 50 mL solution) (a further addition at ca. 50 hrs.).**Figure 6.** Changes in absorption spectra during reaction. O₂ saturated in methanol, 1 atm, 25 °C. [Co(3MeOsalen)] = 5.20×10^{-6} M, [H₂AB]₀ = 3.33×10^{-5} M. No. 4 (20 min.), No. 9 (3 hrs.).

25.0 °C. After most of the substrate was oxidised to azobenzene (in ca. 50 hours), a further addition of hydrazobenzene (0.4606 g/50 mL methanol, 5.00×10^{-2} M) into the reaction mixture was made, Table 5. The absorbance at 437 nm again began to increase, and at a similar rate as before, showing that the catalyst remained active, Figure 5. The spectral changes during the reaction are indicated in Figure 5.

Figure 6 shows the time dependence of the changes in the absorption spectrum during the oxidation of hydrazobenzene (3.33×10^{-5} M) with Co(3MeOsalen) (5.20×10^{-6} M) under oxygen at 25.0 °C. The band at 254 nm decreases with time in Figure 6a, due to the oxidation of hydrazobenzene, while

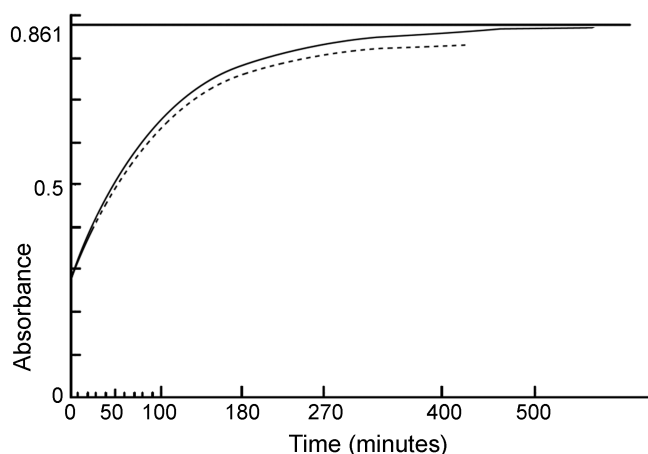


Figure 7. Plot of absorbance A (at 315 nm) against time, O_2 saturated in methanol, 1 atm, 25 °C. $[Co(3MeOsalen)] = 5.67 \times 10^{-6}$ M, $[H_2AB]_0 = 3.26 \times 10^{-3}$ M. Solid curve, experimental; broken curve, calculated for pseudo-first order kinetics as described in the text.

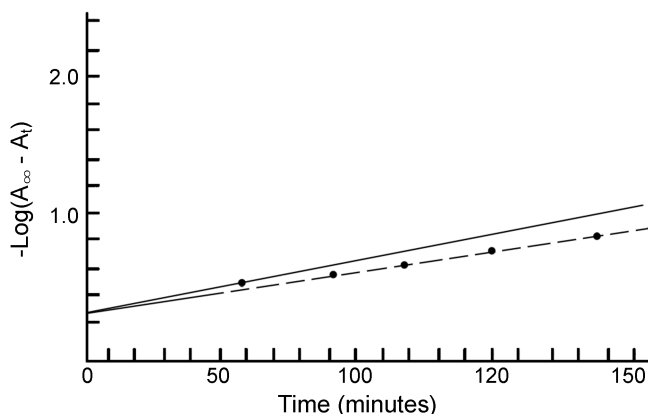


Figure 8. Plot of $-\log(A_\infty - A_t)$ against time, O_2 saturated methanol, 25.0 °C, $\lambda = 315$ nm. $[Co(3MeOsalen)] = 5.67 \times 10^{-6}$ M, $[H_2AB] = 3.26 \times 10^{-5}$ M. $A_\infty = 0.861$. Solid curve: observed value; Dotted line: 1st order kinetics calculated (rate constant $k = 3.33 \times 10^{-4} \text{ sec}^{-1}$).

bands at 315 nm and 437 nm (see Figure 4), increase due to the formation of *trans*-azobenzene in Figures 6-a, b. During the oxidation reaction of hydrazobenzene, *trans*-azobenzene was exclusively produced, as indicated by the absorption spectra. The *cis*-isomer, which would have absorption maxima at 298 nm and 425 nm, was not detected, Figure 6. There is an isosbestic point at 280 nm, and in particular is no new band at 281 nm. Hence the reaction product is *trans*-azobenzene, with negligible production of *cis*-isomer.

Kinetic measurements were made at 315 nm, Figure 7. A typical curve of absorbance A versus time t is shown in Figure 7. Plots of $-\log(A_\infty - A)$ against time were found to be curved after approximately one half-life, 60 minutes, indicating deviation from pseudo first order kinetics. Figure 7 and 8 include a pseudo-first order curve calculated to fit the earlier part of the data. Comparison with the experimental data, Table 6, shows that the reaction appears to go faster as reaction proceeds than would be expected for a simple first order reaction. This could be due to the oxidation of hydrazobenzene by the

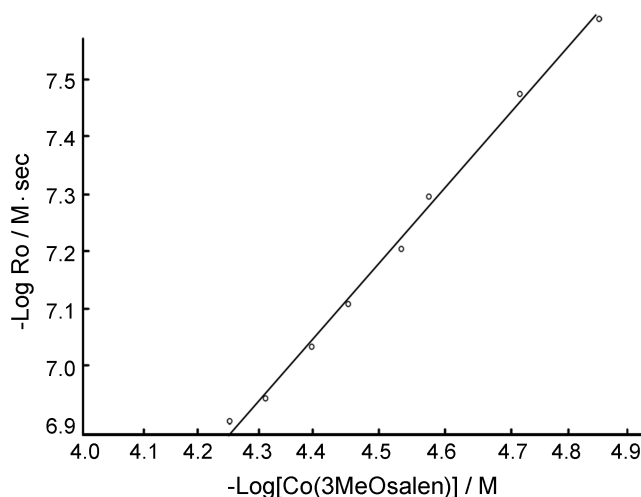


Figure 9. Plot of $-\log R_0$ against $\log[Co(3MeOsalen)]_T$. O_2 saturated methanol, 1 atm, 25 °C, $\lambda = 315$ nm. The line is drawn with slope 1.00. $[Co(3MeOsalen)]_T = 1.47 \times 10^{-5}$ M – 5.57×10^{-5} M. $[H_2AB]_0 = 4.11 \times 10^{-4}$ M.

Table 6. $\log(A_\infty - A_t)$ values compared with first order kinetics

Time/min	Absorbance (observed)	$-\log(A_\infty - A_t)$	Absorbance (Calculated)	$-\log$ (1st order)
0	0.306	0.256	0.306	0.256
10	0.349	0.291	0.349	0.291
20	0.395	0.332	0.395	0.332
30	0.438	0.374	0.438	0.374
60	0.549	0.506	0.537	0.489
90	0.633	0.642	0.615	0.609
120	0.696	0.783	0.675	0.730
150	0.744	0.932	0.717	0.842
180	0.776	1.07	0.752	0.963
2106	0.861			

O_2 saturated methanol, 25.0 °C, $\lambda = 315$ nm. $A_\infty = 0.861$, $[Co(3MeOsalen)] = 5.67 \times 10^{-6}$ M, $[H_2AB] = 3.26 \times 10^{-5}$ M.

hydrogen peroxide produced.¹⁸ We have demonstrated that hydrogen peroxide (8.29×10^{-3} M) reacted with hydrazobenzene (3.88×10^{-4} M) employing the initial rate method, Table 7. The maximum possible rate for the oxidation of hydrazobenzene by hydrogen peroxide in the catalysed reaction would be when half the hydrazobenzene had been oxidised, equation (3). Assuming that the initial rate R_0 is linear (first order) in hydrazobenzene and hydrogen peroxide concentration, the initial rate at $[H_2AB] = [H_2O_2] = 1.63 \times 10^{-5}$ M will be $9.33 \times 10^{-14} \text{ M sec}^{-1}$ which is given by

$$R_0 = \frac{1.13 \times 10^{-9} \text{ M sec}^{-1}}{8.29 \times 10^{-3} \text{ M } (H_2O_2)} \times 1.63 \times 10^{-5} \text{ M } (H_2O_2) \times \frac{1.63 \times 10^{-5} \text{ M } (H_2AB)}{3.88 \times 10^{-4} \text{ M } (H_2AB)}$$

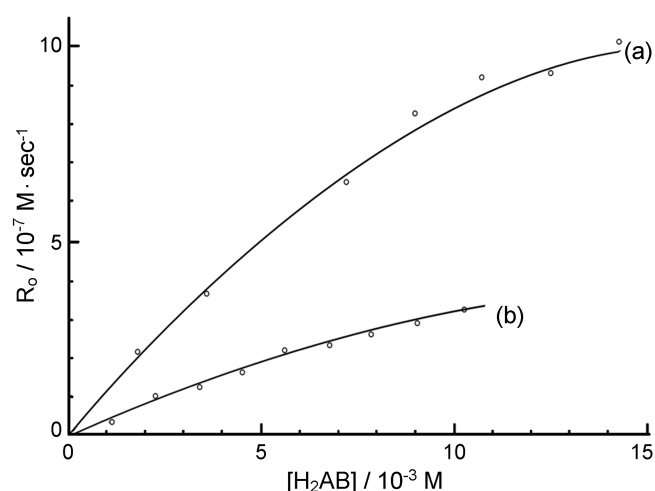
which is obtained, Table 7. This is much less than the initial rate observed ($2.74 \times 10^{-9} \text{ M} \cdot \text{sec}^{-1}$) in the catalysed reaction, Table 7.

To avoid this complication, initial rates R_0 , equation (4)

Table 7. Effect of varying H₂O₂ concentration on the oxidation of hydrazobenzene in O₂ saturated methanol at 25.0 °C

[H ₂ O ₂]/10 ⁻² M	(dA/dt) ₀ /10 ⁻⁴ sec ⁻¹	R ₀ /10 ⁻⁹ M sec ⁻¹
0	0.229	1.61
0.829	0.389	2.74
4.15	1.04	7.32
5.80	1.44	10.1
8.29	2.06	14.5

$\lambda = 315$ nm ($\epsilon(\text{H}_2\text{AB}) = 1.89 \times 10^3 \text{ M}^{-1}\text{cm}^{-1}$, $\epsilon(\text{AB}) = 1.61 \times 10^4 \text{ M}^{-1}\text{cm}^{-1}$, $[\text{H}_2\text{AB}]_0 = 3.88 \times 10^{-4} \text{ M}$, $\Delta\epsilon^{-1} = 7.04 \times 10^{-5} \text{ M}\cdot\text{cm}$, $R_0 = \Delta\epsilon^{-1} (\text{dA}/\text{dt})_0$)

**Figure 10.** Plots of initial rate R_0 against $[\text{H}_2\text{AB}]$. Curve (a) O₂ saturated, Curve (b) air saturated, methanol, 1 atm, 25 °C, $\lambda = 315$ nm and 437 nm. $[\text{Co}]_{\text{T}} = 7.43 \times 10^{-6} \text{ M}$.

were calculated from slopes of tangents at $t = 0$:

$$R_0 = l^{-1} \cdot (\Delta\epsilon)^{-1} \cdot (\text{dA}/\text{dt})_0 \quad (4)$$

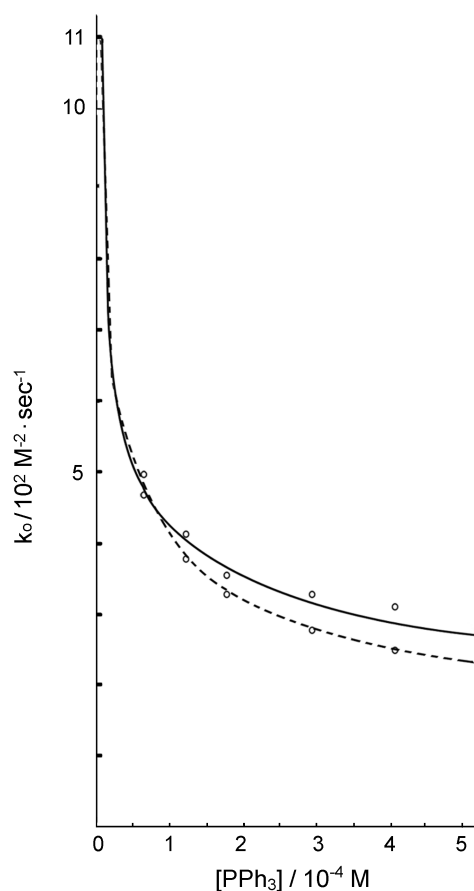
which is derived from $A = \epsilon l$ where l is the path length and $\Delta\epsilon^{-1} = 7.04 \times 10^{-5} \text{ M}^{-1}\cdot\text{cm}$ obtained from intercept with log R_0 against log $(\text{dA}/\text{dt})_0$.

The log of the initial rate is plotted against the log of the Co(3MeOsalen) concentration, Figure 9. The slope of this

Table 8. Effect of varying $[\text{Co}(3\text{MeOsalen})]$ concentration on the oxidation of hydrazobenzene in O₂ saturated methanol at 25.0 °C

$[\text{Co}(3\text{MeOsalen})]$ /10 ⁻⁵ M	(dA/dt) ₀ /10 ⁻⁴ sec ⁻¹	$R_0/10^{-8}$ M·sec ⁻¹	$-\log R_0/$ M·sec ⁻¹	$-\log[\text{Co}(3\text{MeO}$ salen)]/M
0	0.305	0.215	8.67	—
1.47	4.00	2.82	7.55	4.83
2.05	5.53	3.89	7.41	4.69
2.64	7.44	5.24	7.28	4.58
3.22	9.50	6.69	7.17	4.49
3.81	11.5	8.09	7.09	4.42
4.39	13.5	9.50	7.02	4.36
4.98	15.7	11.1	6.95	4.30
5.57	17.2	12.1	6.92	4.25

$\lambda = 315$ nm ($\epsilon(\text{H}_2\text{AB}) = 1.89 \times 10^3 \text{ M}^{-1}\cdot\text{cm}^{-1}$, $\epsilon(\text{AB}) = 1.61 \times 10^4 \text{ M}^{-1}\cdot\text{cm}^{-1}$, $[\text{H}_2\text{AB}] = 4.11 \times 10^{-4} \text{ M}$, $R_0(\text{initial rate}) = \Delta\epsilon^{-1} \cdot (\text{dA}/\text{dt})_0$, $\Delta\epsilon^{-1} = 7.04 \times 10^{-5} \text{ M}\cdot\text{cm}$.)

**Figure 11.** Plots of k against $[\text{PPh}_3]$. O₂ saturated methanol, 25.0 °C, $\lambda = 315$ nm. $[\text{Co}(3\text{MeOsalen})] = 4.78 \times 10^{-5} \text{ M}$, $[\text{H}_2\text{AB}] = 1.95 \times 10^{-4} \text{ M}$, Solid curve: experimental value; dotted curve: theoretical value.

plot is 1.00, Table 8, which shows that the reaction is first order in catalyst, equation (5). The dependence of rate on total cobalt concentration $[\text{Co}]_{\text{T}}$ is linear, over the range

$$R_0 \propto [\text{Co}(\text{II})] \quad (5)$$

$[\text{Co}]_{\text{T}} = (1.5\text{--}5.6) \times 10^{-5} \text{ M}$, Figure 9.

The hydrazobenzene dependence is non-linear, suggesting an equilibrium saturation effect, Figure 10. The oxygen dependence, based on measurements at two concentrations, is also non-linear as discussed below. The initial rate of the oxidation reaction of hydrazobenzene in an O₂ saturated solution is faster than that in air by about three times, for example in the region $[\text{H}_2\text{AB}] = 10 \times 10^{-3} \text{ M}$, Table 2 and 3. The data, Figure 10, show that the initial reaction rates are linear in hydrazobenzene concentration at low concentrations, especially for the reaction in air, as expected for a first order reaction. However, as the hydrazobenzene concentration increases the reaction order in substrate appears to decrease, until above 10^{-2} M hydrazobenzene in oxygen the reaction becomes independent of substrate concentration. This is similar to the behaviour observed in enzyme systems where it would indicate saturation of the catalyst with substrate as the Michaelis-Menten equation.

The reaction was followed with Co(3MeOsalen) ($7.43 \times$

10^{-5} M) and the appropriate ligands: triphenylphosphine (1.91×10^{-2} M), ethylisonicotinate (3.57×10^{-2} M), Table 9. As the ligand triphenylphosphine (1.91×10^{-2} M) was added to the reaction mixture, Table 10, the initial rate was decreased. It was also observed that the colour of the catalytic system changed from red to green. The destruction of catalytic system Co(3MeOsalen)(O₂) could be due to the catalyst becoming coordinated with triphenylphosphine in both Z axis sites of the catalyst. There was a little change in rate when ethylisonicotinate (3.57×10^{-2} M) was added to the reaction mixture, Table 9. However, when a strong σ -donor ligand, pyridine (2.00×10^{-3} M), was added to the reaction mixture of hydrazobenzene, the reaction rate was increased. These ligands could affect dioxygen binding to

the catalytic system Co(3Me Osalen)(O₂) as triphenylphosphine is usually considered to have not only σ -donor but also π -acceptor properties,²⁷ ethylisonicotinate is a σ -donor,¹³ and pyridine a strong σ -donor ligand.

Triphenylphosphine is an interesting ligand as it decreases the rate of the oxidation of hydrazobenzene in methanol. The initial rates, R_0 , of the oxidation of hydrazobenzene with the ligand triphenylphosphine (PPh₃) were measured, Table 10. As the triphenylphosphine concentrations increased, the initial rates were found to decrease. When the initial rates were plotted against the triphenylphosphine concentration, a curve was formed and theoretical values of the initial rates as a dotted curve, Figure 11. The theoretical values of the rates, Table 11, were calculated from equation (6):

$$\text{Rate} = k = \frac{k_1 + k_2 K_1 [P]}{1 + K_1 [P] + K_1 K_2 [P]^2} \quad (6)$$

where $k = (R_0 - k_0[S][O_2]) / [S][O_2][C]_T$

R_0 = initial rate

k_0 = rate constant for autoxidation

$[C]_T$ = total concentration of the catalyst Co(3Me Osalen)

$[S] = [H_2AB]$

$[P] = [PPh_3]$

k_1 = rate constant for the oxidation without PPh₃

k_2 = rate constant for the oxidation with PPh₃

K_1 = equilibrium constant in equation (7)

K_2 = equilibrium constant in equation (8)

Table 9. Ligand effect on the oxidation of hydrazobenzene in O₂ saturated methanol at 25.0 °C

[H ₂ AB] / 10 ⁻³ M	(dA / dt) ₀ / 10 ⁻³ sec ⁻¹			R ₀ / 10 ⁻⁷ M sec ⁻¹		
	MeOH	EIN	PPh ₃	MeOH	EIN	PPh ₃
1.70	4.50	4.50	1.20	3.17	3.17	0.845
3.70	7.40	7.40	2.50	5.21	5.21	1.76
7.30	13.2	12.7	3.40	9.29	8.94	2.39
10.0	18.6	16.8	3.70	13.1	11.8	2.60
14.6	20.8	21.5	4.10	14.6	15.1	2.89

$\lambda = 315$ nm ($\epsilon(H_2AB) = 1.89 \times 10^3$ M⁻¹cm⁻¹), ($\epsilon(AB) = 1.61 \times 10^4$ M⁻¹cm⁻¹), $\lambda = 437$ nm ($\epsilon = 5.09 \times 10^2$ M⁻¹cm⁻¹), $[Co(3MeOsalen)] = 7.43 \times 10^{-5}$ M, Ethylisonicotinate = [EIN] = 3.57×10^{-2} M, $R_0 = \Delta\epsilon_{315}^{-1}(dA/dt)_0$, $\Delta\epsilon_{315}^{-1} = 7.43 \times 10^{-3}$ M⁻¹cm. Triphenylphosphine = [PPh₃] = 1.91×10^{-2} M.

Table 10. Effect of varying triphenylphosphine concentration [PPh₃] on the oxidation of hydrazobenzene [H₂AB] in O₂ saturated methanol at 25.0 °C

[PPh ₃] / 10 ⁻⁴ M	(dA / dt) ₀ / 10 ⁻⁴ sec ⁻¹	R ₀ / 10 ⁻⁸ M·sec ⁻¹	R ₀ ' / 10 ⁻⁸ M·sec ⁻¹	k / 10 ² M ⁻² ·sec ⁻¹	(k-k ₁)10 ² M ⁻² ·sec ⁻¹	[P]/(k-k ₁)/10 ⁻⁷ M ³ ·sec	k ⁻¹ /10 ⁻³ M ² ·sec
0	14.2	9.99	9.99	11.0	0	—	0.909
0.529	6.25	4.40	4.32	4.80	-6.20	0.853	2.19
1.09	5.54	3.90	3.82	4.25	-6.75	1.61	2.36
1.60	4.83	3.40	3.32	3.69	-7.31	2.19	2.71
2.70	4.47	3.15	3.07	3.41	-7.59	3.56	2.93
3.77	4.26	3.00	2.92	3.24	-7.76	4.86	3.09
4.88	3.76	2.65	2.57	2.86	-8.14	5.99	3.49

$k = (R_0 - k_0[S][O_2][C]_T) / [S][O_2][C]_T = 1.11 \times 10^{10} (R_0 - 7.51 \times 10^{-10} M^{-2} \cdot sec^{-1})$, $R_0' = R_0 - k_0[S][O_2]$, $k_0[S][O_2] = 7.51 \times 10^{-10} M \cdot sec^{-1}$ from Figure 2, $[S] = [H_2AB] = 1.95 \times 10^{-4}$ M, $[C]_T = [Co(3MeOsalen)] = 4.78 \times 10^{-5}$ M, $R_0 = \Delta\epsilon_{315}^{-1}(dA/dt)_0$, $\epsilon_{315} = 1.61 \times 10^4$ M⁻¹·cm⁻¹, $\lambda = 315$ nm, $\Delta\epsilon_{315}^{-1} = 7.04 \times 10^{-3}$ M⁻¹cm, $k_1 = 1.10 \times 10^3$ M⁻²·sec⁻¹, $k_2 = 2.69 \times 10^2$ M⁻²·sec⁻¹, $[P] = PPh_3$, $K_1 = 4.56 \times 10^4$ dm³·mol⁻¹, $K_2 = 5.39 \times 10^2$ dm³·mol⁻¹.

Table 11. Theoretical values of the rates calculated from equation (6) using the values of k_1 , k_2 , K_1 , and K_2

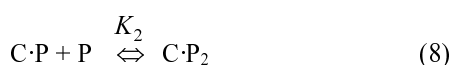
[PPh ₃] / 10 ⁻⁴ M	[P] ² / 10 ⁻⁸	1 + K ₁ [P]	K ₁ K ₂ [P] ²	(k ₁ + k ₂ K ₁ [P])/10 ³	1 + K ₁ [P] + K ₁ K ₂ [P] ²	k / 10 ²
0	0	1	0	1.10	1	11.0
0.529	0.279	3.41	0.0686	1.76	3.48	5.06
1.09	1.19	5.97	0.293	2.45	6.26	3.91
1.60	2.56	8.29	0.629	3.08	8.92	3.45
2.70	7.29	13.3	1.79	4.43	15.1	2.93
3.77	14.2	18.2	3.49	5.75	21.7	2.65
4.88	23.8	23.3	5.85	7.11	29.2	2.43

$k = (k_1 + k_2 K_1 [P]) / (1 + K_1 [P] + K_1 K_2 [P]^2)$, $[P] = [PPh_3]$, $k_1 = 1.10 \times 10^3$ M⁻²·sec⁻¹, $k_2 = 2.69 \times 10^2$ M⁻²·sec⁻¹, $K_1 = 4.56 \times 10^4$ dm³·mol⁻¹, $K_2 = 5.39 \times 10^2$ dm³·mol⁻¹.

Table 12. Rate and Equilibrium Constants at 25 °C

K_N	$0 \pm 10 \text{ M}^{-1}$
k_c	$(2.96 \pm 0.2) \times 10^{-1} \text{ sec}^{-1}$
$\frac{1+K_0[\text{O}_2]}{k_c k[\text{O}_2]}$	$\left\{ \begin{array}{l} (2.05 \pm 0.04) \times 10^{-1} \text{ M} \cdot \text{sec} \text{ ([O}_2\text{]} = 1.96 \times 10^{-3} \text{ M})_a \\ (5.75 \pm 0.2) 10^{-2} \text{ M} \cdot \text{sec} \text{ ([O}_2\text{]} = 9.63 \times 10^{-3} \text{ M})_b \end{array} \right.$
K_0	$(5.42 \pm 0.1) \times 10^1 \text{ M}^{-1}$
K	$(9.33 \pm 0.5) \times 10^3 \text{ M}^{-2}$
K'_N	$(1.72 \pm 0.09) \times 10^2 \text{ M}^{-1}$

$K = K_0 K'_N$. ^aSheehan, W. F., "Physical Chemistry", 2nd. ed., Allyn and Bacon (1970), pp. 285. ^bGjaldbek J. C., Acta Chemica Scandinavica, 6, 623 (1952); Moore (1972).



where C and P are catalyst and triphenylphosphine. The equation (6) was derived from rate law.

The constants k_2 , K_1 , and K_2 were determined by reciprocal plots from equation (6), and k_1 is known to be $1.10 \times 10^3 \text{ M}^{-2} \text{ sec}^{-1}$ when $[\text{P}] = 0$, Table 10.

When $[\text{P}]$ is small, equation (6) reduces to equation (9) as $K_1[\text{P}] \gg K_1 K_2 [\text{P}]^2$

$$k \cong \frac{k_1 + k_2 K_1 \text{P}}{1 + K_1 \text{P}}, \text{ where } \text{P} = [\text{P}]$$

Subtracting k_1 from both sides,

$$\frac{k_1 - k_1}{\text{P}} = \frac{k_2 K_1 - k_1 K_1}{1 + K_1 \text{P}}$$

$$\frac{\text{P}}{k_1 - k_1} = \frac{1}{K_1(k_2 - k_1)} + \frac{\text{P}}{k_2 - k_1} \quad (9)$$

$\text{P} / (k - k_1)$ is plotted against P from equation (9), Figure 12, K_1 and k_2 were obtained graphically, Table 11. When $[\text{P}]$ is large, equation (6) reduces to equation (10) as $k_1 \ll k_2 K_1 [\text{P}]$ and $1 \ll K_1 [\text{P}]$

$$k \cong \frac{k_2 K_1 \text{P}}{K_1 \text{P} + K_1 K_2 \text{P}^2} = \frac{k_2}{1 + K_2 \text{P}}$$

$$\frac{1}{k} = \frac{1}{k_2} + \frac{K_2 \text{P}}{k_2} \quad (10)$$

$1/k$ is plotted against P from equation (10), Figure 13, and K_2 was determined graphically, Table 11. As the theoretical values of the initial rates agreed fairly well with experimental observations, Figure 11, it is suggested that the catalyst $\text{Co}(3\text{MeOsalen})$ was associated with triphenylphosphine which would be a poorer σ donor ligand compared with methanol molecule and the reaction rate therefore decreased. The large K_1 value ($K_1 = 4.56 \times 10^4 \text{ dm}^3 \cdot \text{mol}^{-1}$) means that the equilibrium to $\text{Co}(3\text{MeOsalen})(\text{PPh}_3)$ was soon achieved and was ready to associated with triphenylphosphine and became $\text{Co}(3\text{MeOsalen})(\text{PPh}_3)_2$ which is catalytically inactive and the rates were then expected to decrease quickly.

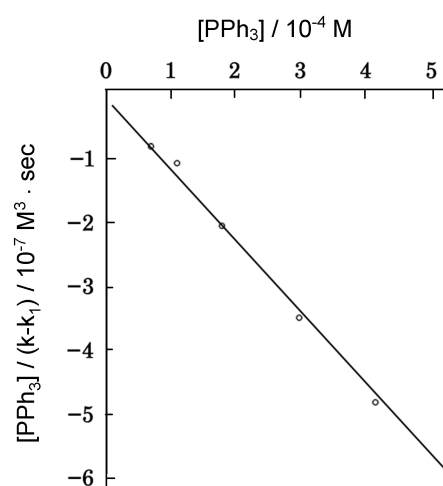


Figure 12. Plot of $[\text{PPh}_3] / (k - k_1)$ against $[\text{PPh}_3]$, when $[\text{PPh}_3]$ is small. O_2 saturated methanol, 25.0 °C, $\lambda = 315 \text{ nm}$, $[\text{Co}(3\text{MeOsalen})] = 4.78 \times 10^{-5} \text{ M}$, $[\text{H}_2\text{AB}] = 1.95 \times 10^{-4} \text{ M}$, $k_1 = 1.10 \times 10^3 \text{ M}^{-2} \cdot \text{sec}^{-1}$, $k_2 = 2.69 \times 10^2 \text{ M}^{-2} \cdot \text{sec}^{-1}$, $K_1 = 4.56 \times 10^2 \text{ M}^4 \cdot \text{dm}^3 \cdot \text{mol}^{-1}$.

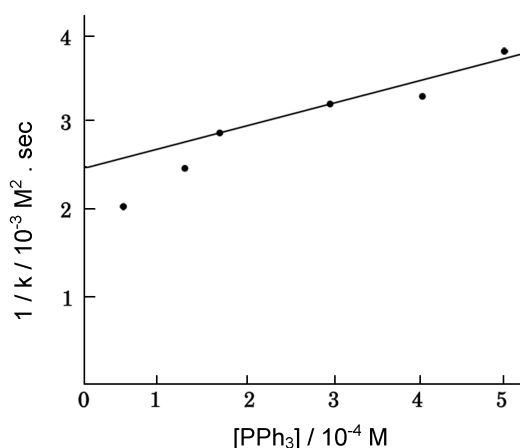
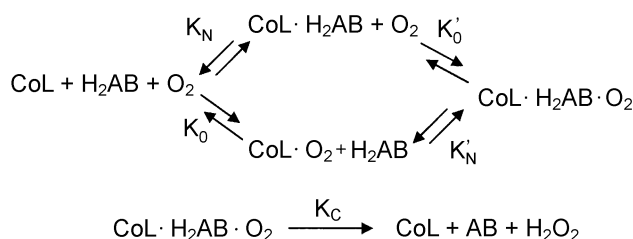


Figure 13. Plot of $1/k$ against $[\text{PPh}_3]$, when $[\text{PPh}_3]$ is large. O_2 saturated methanol, 25.0 °C, $\lambda = 315 \text{ nm}$, $[\text{Co}(3\text{MeOsalen})] = 4.78 \times 10^{-5} \text{ M}$, $[\text{H}_2\text{AB}] = 1.95 \times 10^{-4} \text{ M}$, $K_2 = 5.39 \times 10^2 \text{ dm}^3 \cdot \text{mol}^{-1}$.

Discussion

The data suggest the formation of a ternary complex $\text{CoL} \cdot \text{H}_2\text{AB} \cdot \text{O}_2$ (where $\text{L} = 3\text{MeOsalen}$), Scheme 1.²⁸ For completeness, we introduce stepwise equilibria for the formation of this complex, *via* the two binary complexes $\text{CoL} \cdot \text{H}_2\text{AB}$ and $\text{CoL} \cdot \text{O}_2$:



Scheme 1

Under the experimental conditions

$$[\text{O}_2] > [\text{H}_2\text{AB}] > [\text{CoL}]$$

the rate of reaction is derived as follows: The rate of formation of the product, azobenzene (AB), is given by equation (11).

$$\frac{d[\text{AB}]}{dt} = K_c[\text{CoL} \cdot \text{H}_2\text{AB} \cdot \text{O}_2] \quad (11)$$

The equilibrium constants K_o , K_N , and K'_N are defined in equations (12)-(14).

$$K_o = \frac{[\text{CoL} \cdot \text{O}_2][\text{H}_2\text{AB}]}{[\text{CoL}][\text{H}_2\text{AB}][\text{O}_2]} \quad (12)$$

$$K_N = \frac{[\text{CoL} \cdot \text{H}_2\text{AB}][\text{O}_2]}{[\text{CoL}][\text{H}_2\text{AB}][\text{O}_2]} \quad (13)$$

$$K'_N = \frac{[\text{CoL} \cdot \text{H}_2\text{AB} \cdot \text{O}_2]}{[\text{CoL} \cdot \text{O}_2][\text{H}_2\text{AB}]} \quad (14)$$

From equation (12) and (14), the value of $[\text{CoL} \cdot \text{H}_2\text{AB} \cdot \text{O}_2]$ is given by

$$[\text{CoL} \cdot \text{H}_2\text{AB} \cdot \text{O}_2] = K'_N K_o [\text{CoL}][\text{O}_2][\text{H}_2\text{AB}] \quad (15)$$

The total concentration of the catalyst $[\text{Co}]_T$ is given by equation (16)

$$[\text{Co}]_T = [\text{CoL}] + [\text{CoL} \cdot \text{O}_2] + [\text{CoL} \cdot \text{H}_2\text{AB}] + [\text{CoL} \cdot \text{H}_2\text{AB} \cdot \text{O}_2] \quad (16)$$

Substituting the expressions for various catalyst containing species from equation (12), (13), and (14) yields equation (17)

$$[\text{CoL}] = \frac{[\text{CoL}]_T}{1 + K_o[\text{O}_2] + K_N[\text{H}_2\text{AB}] + K'_N K_o[\text{H}_2\text{AB}][\text{O}_2]} \quad (17)$$

Substituting equation (17) into equation (15) gives:

$$[\text{CoL} \cdot \text{H}_2\text{AB} \cdot \text{O}_2] = \frac{K'_N K_o [\text{Co}]_T [\text{H}_2\text{AB}][\text{O}_2]}{1 + K_o[\text{O}_2] + K_N[\text{H}_2\text{AB}] + K'_N K_o[\text{H}_2\text{AB}][\text{O}_2]} \quad (18)$$

The rate of azobenzene formation is derived from equation (11) and (18):

$$R = \frac{d[\text{AB}]}{dt} = \frac{K_c K [\text{Co}]_T [\text{H}_2\text{AB}][\text{O}_2]}{1 + K_o[\text{O}_2] + K_N[\text{H}_2\text{AB}] + K[\text{H}_2\text{AB}][\text{O}_2]} \quad (19)$$

, where $K = K'_N K_o$. The constants are best determined by a plot of $1/k_o$ versus $1/[\text{H}_2\text{AB}]$ from equation (20):

$$\frac{1}{k_o} = \frac{1}{[\text{H}_2\text{AB}]} \left(\frac{K_o}{k_c K} + \frac{1}{k_c K [\text{O}_2]} \right) + \frac{1}{k_c} \left(1 + \frac{K_N}{K [\text{O}_2]} \right) \quad (20)$$

where $k_o = R / [\text{Co}]_T$ and $K = K'_N K_o = K_o K'_N$. The intercept

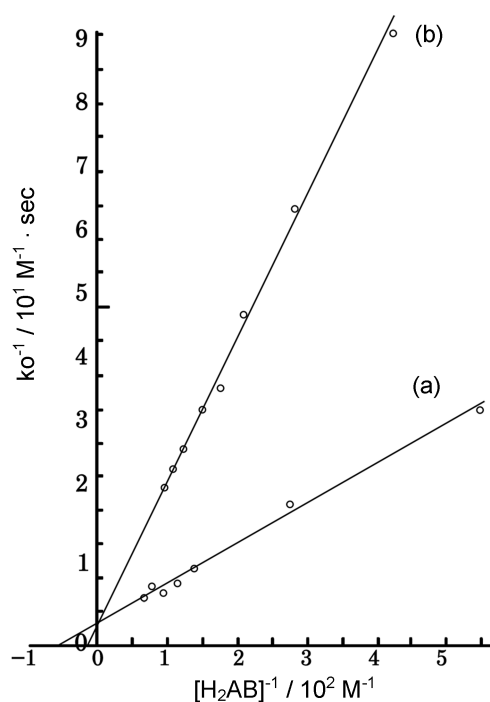


Figure 14. Plots of k_o^{-1} against $[\text{H}_2\text{AB}]_0$. Curve (a) O_2 saturated, Curve (b) air saturated, Methanol, 1 atm, 25 °C. $[\text{Co}]_T = 7.30 \times 10^{-6}$ M.

on the $1/k_o$ axis is:

$$\frac{1}{k_o} = \frac{1}{k_c} \left(1 + \frac{K_N}{K [\text{O}_2]} \right)$$

This is only independent of $[\text{O}_2]$ if K_N is zero. The slope of the plot of $1/k_o$ versus $1/[\text{H}_2\text{AB}]$ is:

$$\frac{k_o}{k_c K} + \frac{1}{k_c K [\text{O}_2]}$$

and it should decrease to a limiting value as the oxygen concentration is increased.

If the kinetic scheme is correct, we expect that plot of the reciprocal of k_o against the reciprocal of the hydrazobenzene concentration at constant $[\text{O}_2]$ will be linear in accordance with equation (20). Figure 14 shows that the plots are linear and it is noteworthy that the plots for different O_2 concentrations should intersect at a single point, with $[\text{H}_2\text{AB}]^{-1} = -K_N$. The intersection point lies within experimental error on the vertical axis. This indicates that the reaction *via* the binary complex cobalt H_2AB ($\text{CoL} \cdot \text{H}_2\text{AB}$) does not occur and the value of k_c may be read from the intersection point, while the slopes of the two lines gives K_o and K . Values of rate and equilibrium constants, with estimated limits of error, are shown in Table 12. The kinetic studies show that a ternary complex $\text{CoL} \cdot \text{H}_2\text{AB} \cdot \text{O}_2$ is involved in the rate determining step.

Possible structures for the ternary complex $\text{CoL} \cdot \text{H}_2\text{AB} \cdot \text{O}_2$ include structure I, structure II, and structure III. To account for the hydrogen abstraction, the structure I with N-H-O bridging seems plausible. However, in a concerted reaction this would be expected to lead to *cis*-azobenzene, which was

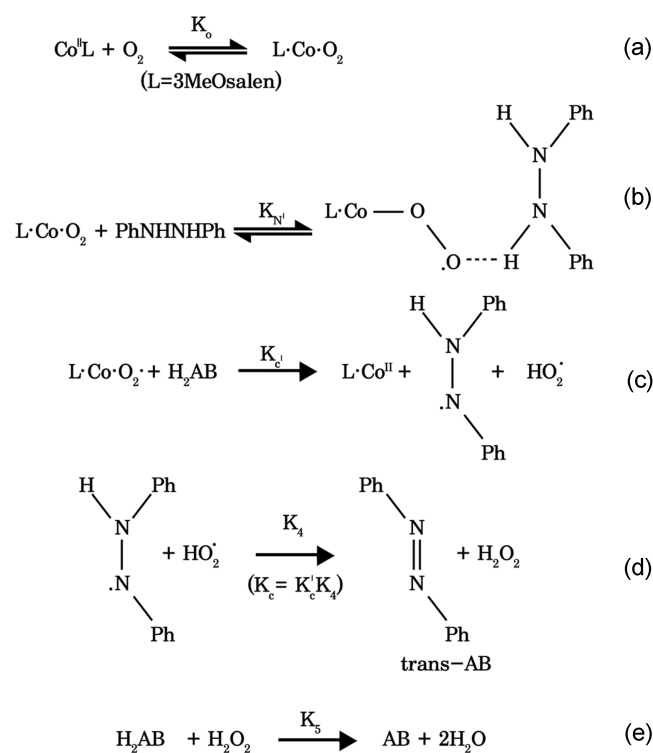
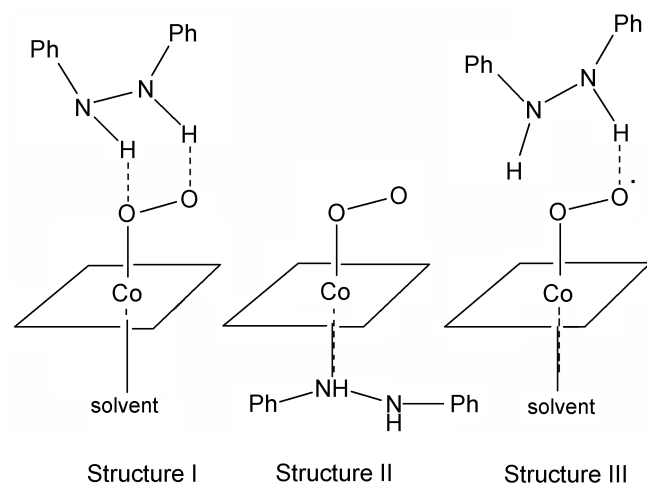


Figure 15. Proposed mechanism for the oxidation of hydrazobenzene by cobalt dioxygen catalyst $\text{Co}(\text{3MeOsalen})(\text{O}_2)$.³²

not observed. The isomerisation of *cis*-azobenzene to the *trans* isomer was also followed at 315 nm, and the reaction rate was very slow and was not catalysed by $\text{Co}(\text{3MeOsalen})$.

The first order rate constant for the isomerisation was found to be $1.28 \times 10^{-6} \text{ sec}^{-1}$ which is much smaller than the rate constant ($3.33 \times 10^{-4} \text{ sec}^{-1}$) for the oxidation of hydrazobenzene calculated from Figure 8. Thus *cis*-azobenzene could not have been the initial product. Structure II is not necessarily the effective reaction intermediate. The situation in which an association complex is detected, but some other species of the same composition, but relatively less stable, is the true reaction intermediate, is paralleled in

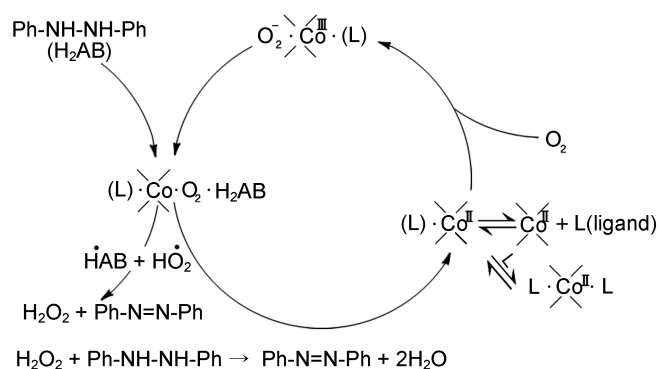


Figure 16. Catalysis cycle for $\text{Co}(\text{3MeOsalen})$ catalysed oxidation of hydrazobenzene, $[\text{H}_2\text{AB}]$ by molecular oxygen.³²

many other reactions *e.g.* electron transfer by the 'dead-end' mechanism.²⁹ The most reasonable intermediate is structure III. Drago's group⁸ proposed hydrogen bonding to the terminal oxygen of the bound dioxygen molecule because the terminal oxygen has more of the unpaired electron density on it.³⁰ The upper limit of K_N is estimated as 10^{-1} M^{-1} while $K'_N = K/K_o = 172 \text{ M}^{-1}$. The difference can be understood if the d_{z^2} electron in the complex is partially delocalised onto the O_2 molecule, so that the effective oxidation state of cobalt is intermediate between Co^{II} and Co^{III} .²⁸

The proposed mechanism is shown in Figure 15. The polar solvent, methanol, coordinates to the cobalt(II) complex and affects the electron density of the d_{z^2} orbital of cobalt, increasing the charge on the dioxygen moiety, equation (a). This causes the abstraction of the hydrogen atom, equation (c). The N-H-O bridging structure III and equation (b) are analogous to that suggested by Savitskii⁹ for isopropanol oxidation and by Beckett³¹ for the 1-phenylethanol oxidation reaction. After abstraction of the hydrogen atom, radicals $\cdot\text{HAB}$ and HO_2^\cdot (hydroperoxy), may be formed, equation (c), and the catalyst regenerated. The formation of the HO_2^\cdot and $\cdot\text{HAB}$ radicals also agrees with Drago's mechanism¹⁵ for the catalysed oxidation of phenol. If *cis*- HAB^\cdot is formed in step (b) it could rearrange rapidly to the *trans* form by rotation about the N-N bond before reacting with HO_2^\cdot to produce *trans*-azobenzene and hydrogen peroxide. According to Beckett and Homer's²¹ proposal, in a related system, the hydrogen peroxide may affect further oxidation of substrate and produce azobenzene and water. The reactions are summarised in the catalytic cycle, Figure 16.

Experimental Section

$\text{H}_2(\text{3MeOsalen})$ was prepared by the method of Diehl *et al.*,³³ 3-methoxysalicylaldehyde (35.5 mmol) was dissolved in hot absolute ethanol (25 mL) and the solution stirred for 30 minutes ethanol. Yield 72%, mp 162-163 °C, as reported. Elemental analysis based on $\text{C}_{18}\text{H}_{20}\text{N}_2\text{O}_4$: calculated C: 65.9, N: 8.5, H: 6.1; found: C 65.6, N: 8.4, H: 6.2.

The catalyst $\text{Co}^{\text{II}}(\text{3MeOsalen})$, was prepared by the method of Diehl *et al.*,³³ as modified by Beckett.³¹ The ligand,

H₂(3MeOsalen) (35.5 mmoles) was dissolved in absolute ethanol (300 mL) and cobalt(II) acetate tetrahydrate (35.5 mmoles) was dissolved in hot water under nitrogen and added dropwise to the solution of the ligand. The pink solution changed to dark red. After cooling, a silver gold precipitate was formed. The product was filtered, washed with ethanol (30 mL) and then water (30 mL), and finally dried in vacua at 180 °C for at least two hours. The colour of the product changed from silver gold to violet. Yield 52%. Elemental analysis based on CoO₄N₂C₁₈H₁₅O₂: calculated: C: 51.80, H: 4.36, N: 6.71; found: C: 52.15, H: 4.74, N: 6.87.

Hydrazobenzene (Aldrich) was always kept in a dry nitrogen glove bag. Dry nitrogen was produced by passing cylinder nitrogen over P₂O₅. Oxygen saturated reaction mixtures were made by bubbling oxygen through the solution for fifteen minutes.

The rates of the reactions were followed by observing absorbance changes against time in the reaction mixtures at a wavelength of 325 nm or 437 nm in 1 cm cells. The reactions were conducted at a tenfold molar excess or more of hydrazobenzene over the cobalt(II) complex. The absorption spectra were measured on a Pye Unicam SP8-200 spectrophotometer.

Acknowledgment. This work was supported by grants from the University of Ulsan, British Council, Piaris Co., Ltd., and the Korea Science and Engineering Foundation. We wish to thank Professor S. F. A. Kettle for helpful discussions.

References

- (a) Pfiffer, P.; Breith, E.; Lubbe, E.; Tsumaki, T. *Justus Liebigs Ann Chem.* **1933**, 503, 84. (b) Kim, H. N.; Lee, H. K.; Lee, S. W. *Bull. Korean Chem. Soc.* **2005**, 26(6), 892. (c) Lee, N. H.; Byun, J. C.; Oh, T.-H. *Bull. Korean Chem. Soc.* **2005**, 26(3), 454.
- Tsumaki, T. *Bull. Chem. Soc. Jpn.* **1938**, 13, 252.
- Jones, R. D.; Summerville, D. A.; Basolo, F. *Chem. Rev.* **1979**, 79, 139.
- Perutz, M. F. *Brit. Med. Bull.* **1976**, 32, 195.
- Adduci, A. J. *Chemtech.* **1976**, 6, 575.
- Martell, A. E.; Niederhoffer, E. C. J. H.; Timmons, J. H. *Chem. Rev.* **1984**, 84, 137.
- Smith, T. D.; Pilbrow, J. R. *Coord. Chem. Rev.* **1981**, 39, 295.
- Drago, R. S.; Corden, B. B. *Acc. Chem. Res.* **1980**, 13, 353.
- Savitskii, A. V. *J. Gen. Chem., USSR* **1974**, 44, 1518.
- Zombeck, A.; Drago, R. S.; Corden, B. B.; Gaul, J. H. *J. Am. Chem. Soc.* **1981**, 103, 7580.
- Nishinaga, A. *Chem. Lett.* **1975**, 273.
- Martell, A. E.; Bedell, S. A. *Inorg. Chem.* **1983**, 22, 364.
- (a) Savitskii, A. V.; Nelyubin, V. I. *J. of General Chem. of the USSR* **1979**, 49, 2028. (b) Kim, J. C.; Lough, A. J. *Bull. Korean Chem. Soc.* **2005**, 26(1), 169.
- (a) Nishinaga, A.; Tomita, H.; Nishizawa, K.; Matsuura, T. *J. Chem. Soc., Dalton* **1985**, 107, 2903. (b) Lee, J.; Choe, J.-I.; Jung, S.; Ham, S. W. *Bull. Korean Chem. Soc.* **2006**, 27(1), 33.
- Drago, R. S.; Corden, B. B.; Perito, R. P. *J. Am. Chem. Soc.* **1985**, 107, 2903.
- (a) Drago, R. S.; Zombeck, A.; Hamilton, U. E. *J. Am. Chem. Soc.* **1982**, 104, 6782. (b) Cho, C. S.; Kim, D. Y.; Shim, S. C. *Bull. Korean Chem. Soc.* **2005**, 26(5), 802.
- Simandi, L. I.; Nemeth, S.; Szeverenyi, Z. *Inorg. Chim. Acta* **1980**, 44, L107.
- Manchot, W.; Herzog, J. *Justus Liebigs Ann. Chem.* **1901**, 318, 331.
- Walton, J. H.; Filson, G. W. *J. Am. Chem. Soc.* **1932**, 54, 3228.
- Kaup, G.; Russell, G. A. *Chem. Ber.* **1968**, 101, 1729.
- Homer, R. B.; Beckett, M. A. *Inorg. Chim. Acta* **1986**, 115, L25.
- Waters, W. A. *Mechanism of Oxidation of Organic Compounds*; Wiley: London, 1964.
- Kochi, J. K.; Sheldon, R. A. *Adv. Catal.* **1976**, 25, 272.
- Hinshelwood, C.; Blackadder, D. A. *J. Chem. Phys.* **1957**, 2898.
- Wolf, A. J. *Mol. Struct.* **1980**, 67, 89.
- (a) Jaffe, H. H.; Orchin, M. *Theory and Applications of Ultraviolet Spectroscopy*; John Wiley: London, 1966; p 430. (b) Gerson, F.; Heilbronner, E.; Van-Veen, A.; Wepster, B. M. *Helv. Chim. Acta* **1960**, 43, 1889.
- (a) Yamamoto, H.; Takayanagi, T.; Kwan, T. *Bull. Chem. Soc. Jpn.* **1975**, 48, 2618. (b) Habibi-Yangjeh, A.; Nooshyar, M. *Bull. Korean Chem. Soc.* **2005**, 26(1), 139.
- Homer, R. B.; Cannon, R. D.; Kim, S. S. B. *Bull. Korean Chem. Soc.* **1985**, 6, 115.
- Rosenheim, L.; Speiser, D.; Heim, A. *Inorg. Chem.* **1974**, 13, 1571.
- Dori et al. *J. Am. Chem. Soc.* **1975**, 97, 3846.
- Beckett, M. A., *Ph. D. Thesis*, University of East Anglia, 1981.
- Kim, S. S. B., *Ph. D. Thesis*, University of East Anglia, 1987.
- Diel, H.; Liggett, L. M.; Hach, C. C.; Harrison, G. C. *Iowa State Coll. Jour. Science* **1947**, 22, 110.